Electronic Supplementary Material (ESI) for Journal of Materials Chemistry A.

Supporting Information

Revealing the role of aniline in assisting SnO_2 electrocatalytic CO_2 reduction to HCOOH: via the perspective of reaction pathway

Yuning Zhang, [ab] Hao Jiang,[ac] Kangpeng Wang,[b] Dongfang Niu,[a*] and Xinsheng Zhang [a*]

[a] State Key Laboratory of Chemical Engineering, School of Chemical Engineering, East China University of Science and Technology, Shanghai 200237, China

[b] State Key Laboratory of High Field Laser Physics and CAS Center for Excellence in Ultra-intense Laser Science, Shanghai Institute of Optics and Fine Mechanics, Chinese Academy of Sciences, Shanghai 200237, China

[c] Petroleum Processing Research Center, School of Chemical Engineering, East China University of Science and Technology, Shanghai 200237, China

*Corresponding author: dfniu@ecust.edu.cn (D. Niu); xszhang@ecust.eud.cn (X. Zhang)

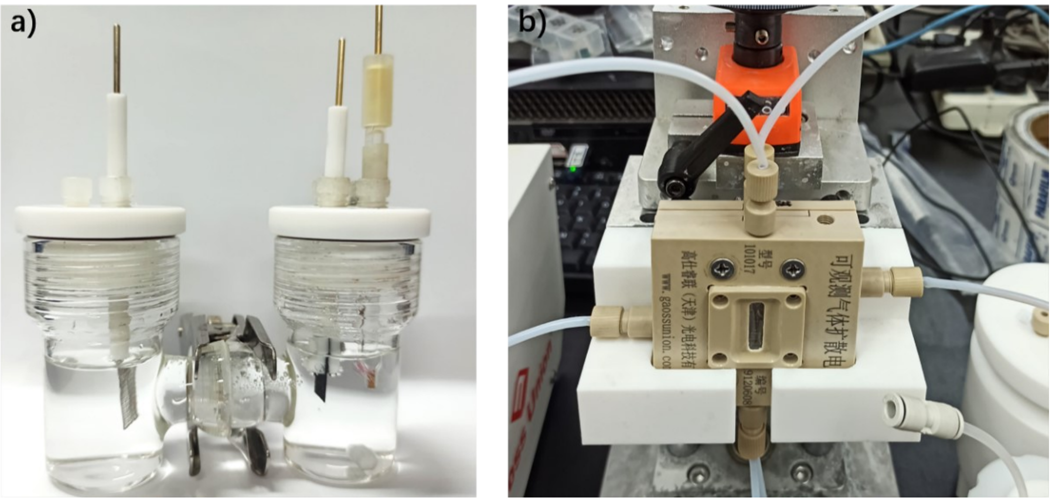

Fig. S1. Pictures of (a) H-type cell and (b) flow cell with an observable gas diffusion electrode.

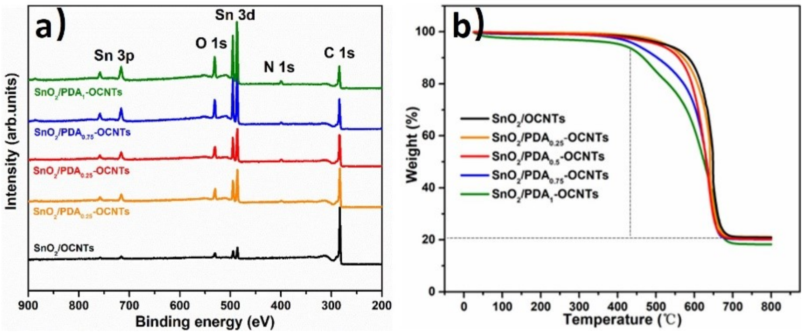

Fig. S2. (a) XPS survey spectra of SnO_2/OCNTs, SnO_2/$PDA_{0.25}$-OCNTs, SnO_2/$PDA_{0.5}$-OCNTs, SnO_2/$PDA_{0.75}$-OCNTs, and SnO_2/PDA_1-OCNTs. (b) Weight loss curves of SnO_2/OCNTs, SnO_2/$PDA_{0.25}$-OCNTs, SnO_2/$PDA_{0.5}$-OCNTs, SnO_2/$PDA_{0.75}$-OCNTs, and SnO_2/PDA_1-OCNTs.

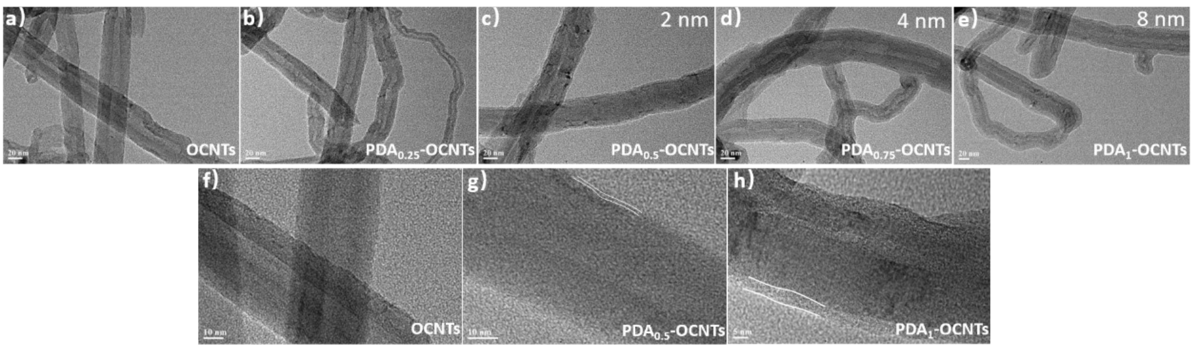

Fig. S3. TEM images of (a) OCNTs, (b) $PDA_{0.25}$-OCNTs, (c) $PDA_{0.5}$-OCNTs, (d) $PDA_{0.75}$-OCNTs, and (e) PDA_1-OCNTs. HR-TEM images of (a) OCNTs, (b) $PDA_{0.5}$-OCNTs, (c) PDA_1-OCNTs.

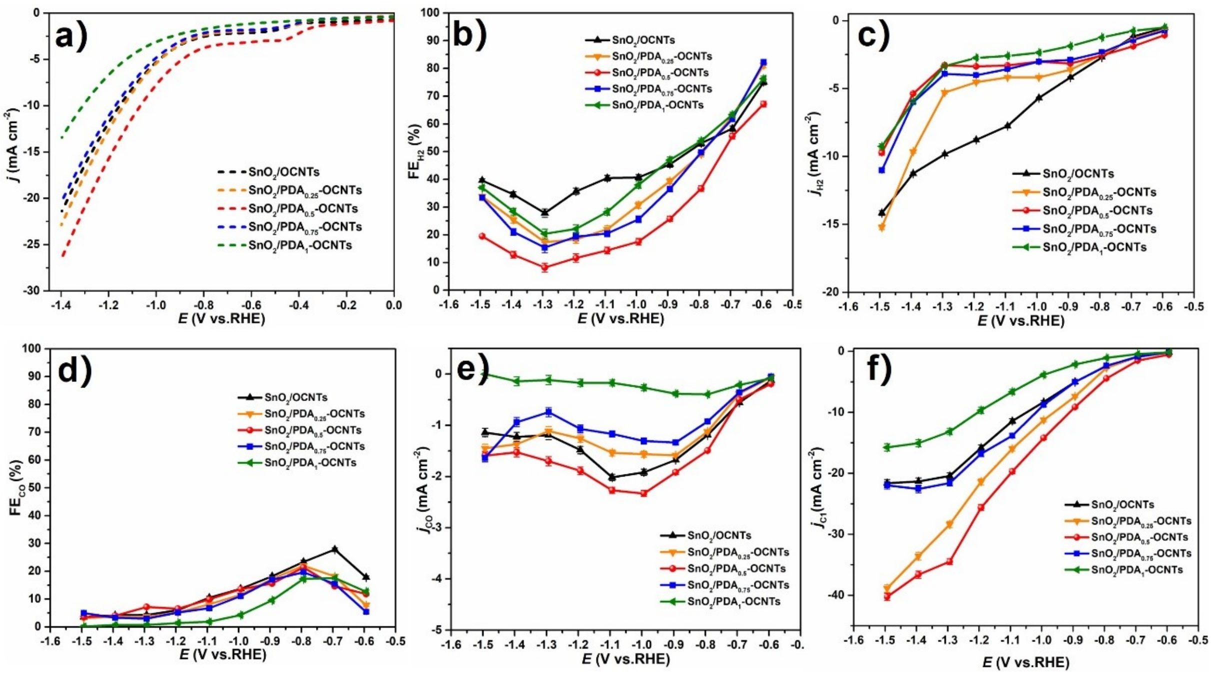

Fig. S4. (a) LSV curves obtained in 0.1 M $KHCO_3$ electrolytes saturated with N_2, (b) Faradaic efficiencies of H_2, (c) partial current densities of H_2, (d) Faradaic efficiencies of CO, (e) partial current densities of CO, and (f) current densities of total C1 products over as-prepared catalysts at different applied potentials.

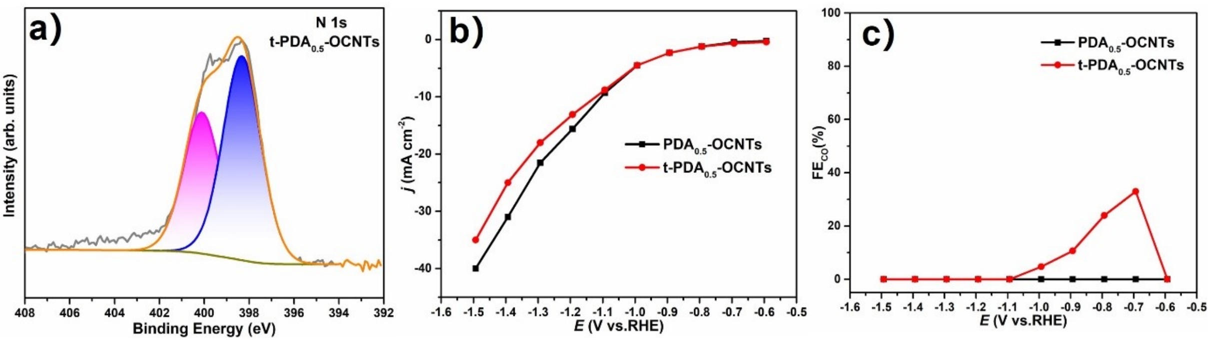

Fig. S5. (a) N 1s XPS spectrum of t-$PDA_{0.5}$-OCNTs. (b) Current densities and (c) Faradaic efficiencies of $PDA_{0.5}$-OCNTs and t-$PDA_{0.5}$-OCNTs at different applied potentials.

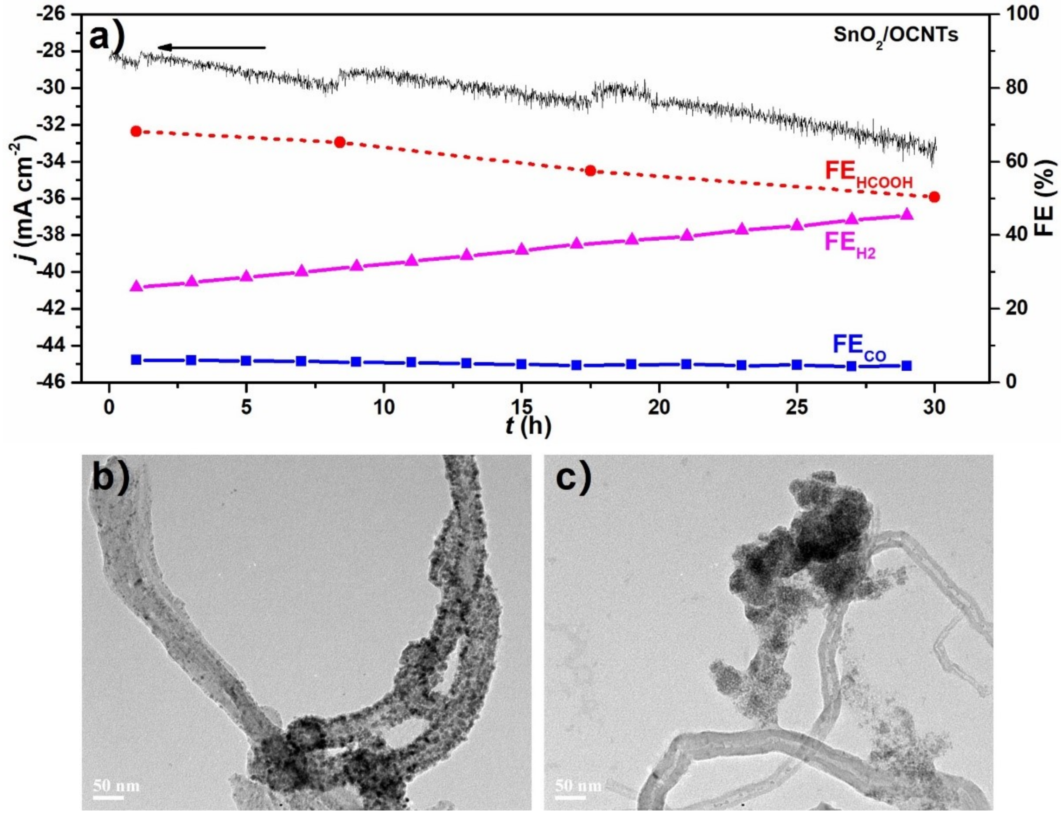

Fig. S6. (a) Stability tests of SnO_2/OCNTs at -1.29 V. TEM images of (b) SnO_2/$PDA_{0.5}$-OCNTs and (c) SnO_2/OCNTs after stability tests.

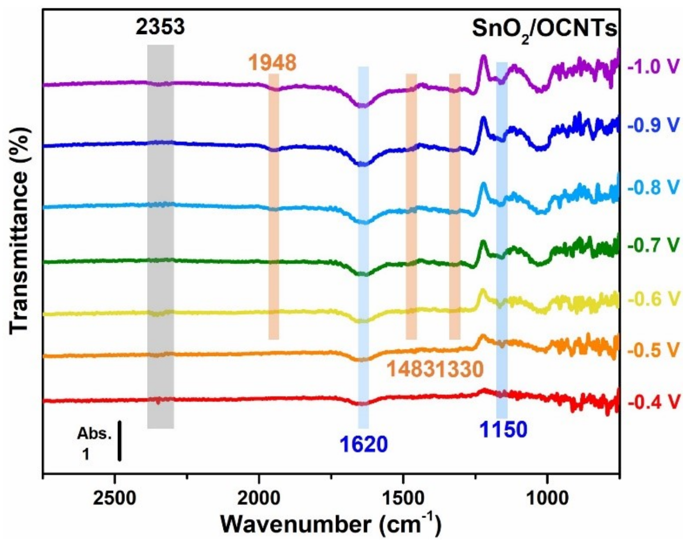

Fig. S7. *In-situ* FT-IR spectra of SnO_2/OCNTs at different applied potentials.

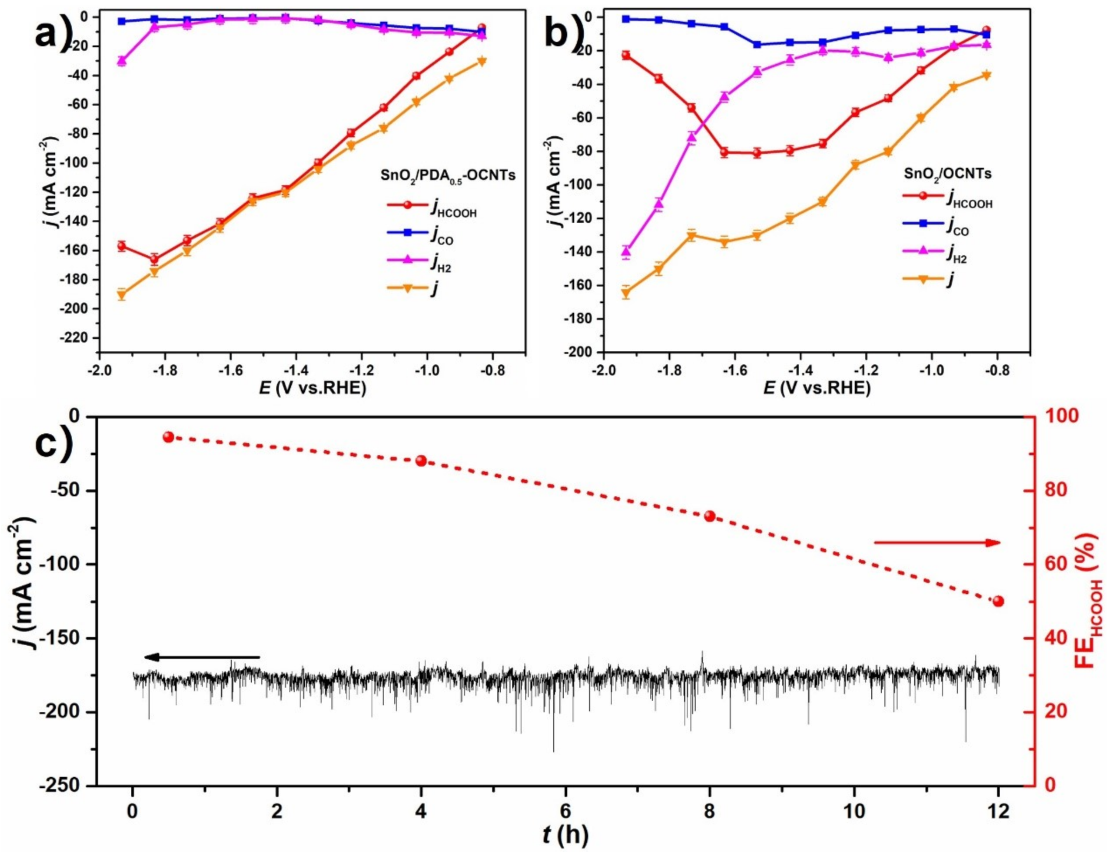

Fig. S8. Current densities over (a) SnO_2/$PDA_{0.5}$-OCNTs and (b) SnO_2/OCNTs at different applied potentials. (c) Stability tests over SnO_2/$PDA_{0.5}$-OCNTs at -1.83 V in the flow cell with 1 M $KHCO_3$.

Table. S1. The contents of N elements of as-prepared catalysts by XPS

Samples	**N content (at.%)**
SnO_2/OCNTs	/
SnO_2/$PDA_{0.25}$-OCNTs	2.62
SnO_2/$PDA_{0.5}$-OCNTs	3.49
SnO_2/$PDA_{0.75}$-OCNTs	3.93
SnO_2/PDA_1-OCNTs	6.64

Table. S2. Contents of elements in the carriers

Samples	**N content (at.%)**	**O content (at.%)**	**C content (at.%)**
OCNTs	/	7.09	92.91
$PDA_{0.25}$-OCNTs	5.35	7.64	87.01
$PDA_{0.5}$-OCNTs	7.51	8.13	84.36
$PDA_{0.75}$-OCNTs	9.45	7.38	83.17
PDA_1-OCNTs	11.2	4.67	84.13

Table. S3. Summary of the reported CO_2ER performance over SnO_2-based electrocatalysts

Catalysts	Electrolytes	Potential at FE_{max} (V vs. RHE)	FE_{HCOOH} (%)	j_{HCOOH} ($mA\ cm^{-2}$)	Stability (h)	Ref.
$SnO_2/PDA_{0.5}$-CNTO	0.1 M $KHCO_3$	-1.29	89	-32	36	This work
$SnO_2/PDA_{0.5}$-CNTO	1 M $KHCO_3$	-1.83	95	-166	12	This work
Vo-rich SnO_2	0.5 M $KHCO_3$	-1.1	~ 60	-40	30	[54]
SnO_2@N-CNW	0.5 M $NaHCO_3$	-0.8	90	-13.5	20	[55]
NW-SnO_2	0.5 M $KHCO_3$	-1.0	87.4	-22	18	[56]
SnO_2⊃NC@EEG	0.1 M $KHCO_3$	-1.2	81.2	-11	10	[57]
Sn/CN-0.1	0.1 M $KHCO_3$	-0.9	96	-3.42	10	[58]
SnO_2 nanosheet	0.1 M $KHCO_3$	-1.01	85	-12.75	/	[59]
mSnO_2 NTs-350	0.5 M $KHCO_3$	-1.3	90	-9	12	[60]
VO-rich N-SnO_2 NS	0.1 M $KHCO_3$	-0.9	83	~ -6.7	10	[61]
SnO_2-CNT pH-11	0.5 M $KHCO_3$	-0.77	76	~ -3.5	10	[62]
VO-SnO_x/CF-40	0.1 M $KHCO_3$	-1.0	86	-30	8	[63]
CNT#SnO_2 NDs	0.1 M $KHCO_3$	-0.9	70	-5.3	24	[64]
SnO_2/OC	0.1 M $KHCO_3$	-1.0	75	-15	8	[65]
NRS-SnO	1 M KOH	-0.7	87	-330	/	[66]